Hindawi
Oxidative Medicine and Cellular Longevity
Volume 2021, Article ID 6669787, 15 pages
https://doi.org/10.1155/2021/6669787

Research Article

Activation of Nurr1 with Amodiaquine Protected Neuron and Alleviated Neuroinflammation after Subarachnoid Hemorrhage in Rats

Huaijun Chen, Xiaobo Yu, Libin Hu, Yucong Peng, Qian Yu, Hang Zhou, Chaoran Xu, Hanhai Zeng, Yang Cao, Jianfeng Zhuang, Xiongjie Fu, Guoyang Zhou, Jianru Li, Feng Yan, Lin Wang, Gao Chen, and Jingyin Chen

Department of Neurosurgery, The Second Affiliated Hospital of Zhejiang University School of Medicine, China

Correspondence should be addressed to Gao Chen; d-chengao@zju.edu.cn and Jingyin Chen; cjyaway@zju.edu.cn

Received 11 October 2020; Revised 18 January 2021; Accepted 29 January 2021; Published 10 February 2021

Academic Editor: Robert Ostrowski

Copyright © 2021 Huaijun Chen et al. This is an open access article distributed under the Creative Commons Attribution License, which permits unrestricted use, distribution, and reproduction in any medium, provided the original work is properly cited.

Background. Nurr1, a member of the nuclear receptor 4A family (NR4A), played a role in neuron protection, anti-inflammation, and antioxidative stress in multidiseases. We explored the role of Nurr1 on subarachnoid hemorrhage (SAH) progression and investigated the feasibility of its agonist (amodiaquine, AQ) as a treatment for SAH. *Methods*. SAH rat models were constructed by the endovascular perforation technique. AQ was administered intraperitoneally at 2 hours after SAH induction. SAH grade, mortality, weight loss, neurological performance tests, brain water content, western blot, immunofluorescence, Nissl staining, and qPCR were assessed post-SAH. In vitro, hemin was introduced into HT22 cells to develop a model of SAH. *Results*. Stimulation of Nurr1 with AQ improved the outcomes and attenuated brain edema. Nurr1 was mainly expressed in neuron, and administration of AQ alleviated neuron injury in vivo and enhanced the neuron viability and inhibited neuron apoptosis and necrosis in vitro. Besides, AQ reduced the amount of IL-1β^{+}Iba-1^{+} cells and inhibited the mRNA level of proinflammatory cytokines (IL-1β and TNF-α) and the M1-like phenotype markers (CD68 and CD86). AQ inhibited the expression of MMP9 in HT22 cells. Furthermore, AQ reduced the expression of nuclear NF-κB and Nurr1 while increased cytoplasmic Nurr1 in vivo and in vitro. *Conclusion*. Pharmacological activation of Nurr1 with AQ alleviated the neuron injury and neuroinflammation. The mechanism of antineuroinflammation may be associated with the Nurr1/NF-κB/MMP9 pathway in the neuron. The data supported that AQ might be a promising treatment strategy for SAH.

1. Introduction

Subarachnoid hemorrhage (SAH), a subtype of stroke, mainly caused by the intracranial aneurysm rupture, is characterized by high mortality and morbidity rate [1]. Although accounting for approximately 5%-10% of all strokes, the harm SAH caused was more than that of ischemic stroke, as it tended to affect the younger adults resulting in a disruption of productive lives [2]. Despite great efforts made in preclinical studies and clinical trials, the outcome of patients with SAH remains unacceptably poor, which remainders us to reveal the underlying mechanisms behind SAH and explore and develop reliable therapeutic targets.

Nurr1 (NR4A2), belonging to the nuclear receptor 4A family (NR4A), was an orphan nuclear receptor as no endogenous ligands [3]. In the beginning, quantities of studies paid attention to the role of Nurr1 in Parkinson's disease (PD), demonstrating it not only promoted the maturation of dopaminergic neurons and maintained their survival [4–6] but also promoted the transformation of astrocytes into functional dopaminergic neurons [7, 8], which was considered to be a promising therapeutic target for PD. Indeed, Nurr1 was widely expressed throughout the brain, not only limited in the midbrain dopaminergic neuron area [9]. It is reasonable to believe that Nurr1 may play important roles beyond dopaminergic neurons. Recently, researchers have confirmed the neuron

protective, anti-inflammatory, and antioxidative stress role of Nurr1 in nondopaminergic neuron areas and various diseases, including but not limited to multiple sclerosis [10], Alzheimer's disease (AD) [11], and ischemic stroke [12, 13]. However, the role of Nurr1 in SAH-related pathology has not previously been reported.

Drug repurposing, a strategy to explore new medical indications of approved drugs, provides an attractive and alternative choice to develop new treatment for diseases outside the original scope, as it makes use of the advantage of "old" drugs: reduction of the risk of failure, the time frame of development, and investment [14]. Especially during the epidemic of coronavirus disease 2019 (COVID-19), drug repurposing has been a priority for developing effective drugs and has been made a few efforts [15].

Amodiaquine (AQ) was an antimalarial drug approved by the FDA [16]. Since AQ was first identified as an agonist of Nurr1 through direct interaction with its ligand-binding domain in 2015 [17], pharmacological activation of Nurr1 with AQ had been applied in various brain diseases, including PD [17, 18], AD [11], and intracellular hemorrhage [19], which showed a powerful anti-inflammatory and neurological repair effects. Herein, we speculated that Nurr1 might play an important role in SAH progression, and stimulation of Nurr1 with AQ might be a promising treatment strategy based on the above evidence.

2. Materials and Methods

2.1. SAH Model. Sprague-Dawley rats (male, 300–350 g) were purchased from SLAC Laboratory Animal (Shanghai, China). The rats were housed in stable temperature and humidity animal quarters with a 12 hr day/night cycle and free access to clean water and food ad libitum. All procedures involved in rats were in strict accordance with the guidelines of the National Institutes of Health on the care and use of animals and were approved by the Institutional Animal Care and Use Committee of Zhejiang University.

The experimental SAH model was constructed using the endovascular perforation technique as our previously described studies [20]. Briefly, rats were anesthetized by intraperitoneal injection of 40 mg/kg pentobarbital. After exposing and dissecting the left external carotid artery (ECA), a 4-0 nylon suture was inserted into ECA, marched along the internal carotid artery (ICA) until feeling the resistance, and then pushed into 2-3 mm to perforate the bifurcation between the anterior cerebral artery and middle cerebral artery. The rats were randomly divided into the sham, SAH+vehicle, and SAH+AQ groups. In the sham group, the same surgical procedure was executed except for perforation. 2 hours after SAH induction, rats in the SAH+AQ group were injected AQ (40 mg/kg, MedChemExpress, USA, Cat. No. HY-B1322B) intraperitoneally once daily [19], while the other groups (sham and SAH) were subjected to vehicles (ultrapure water) with equal dosage.

SAH grade after a 24 h operation was assessed as follows: the basal cistern was divided into 6 parts, and each was graded 0-3 according to the amount of blood clot [21]. A total score was calculated by adding the score of each segment. Weight loss was calculated as follows: bodyweight after a 24 h operation minus before the operation and then divided the weight before the operation.

2.2. Neurological Behavior Analysis. Neurological performance after a 24 h operation was evaluated via modified Garcia scoring system [22] and beam walking test [23, 24]. Modified Garcia scoring system included spontaneous activity (0-3), movement symmetry of 4 limbs (0-3), forelimb outstretching (0-3), climbing (1-3), body proprioception (1-3), and response to vibrissae touch (1-3). Then, rats were put on a narrow beam within 1 min and the scores were assessed for beam walking test (0-4).

2.3. Brain Water Content. Rats were sacrificed at 24 h after the operation, and the brains were soon removed and separated into 4 segments (the left hemisphere, right hemisphere, cerebellum, and brain stem). Each segment was weighed quickly to obtain the wet weight (WW) and then seasoned in the dry baths at 105°C for 72 h to get the dry weight (DW). The water content of each segment was calculated based on the following formula: $[(\mathrm{WW} - \mathrm{DW})/\mathrm{WW}] * 100\%$.

2.4. Histological Stain Analysis. Rats were anesthetized, sacrificed, and perfused sufficiently with 4% paraformaldehyde (PFA, dissolved in 0.1 M PBS). The brains were immediately collected and fixed in 4% PFA for 48 h and then dehydrated in a 30% sucrose solution until sinking into the bottom of the bottle. The brains were embedded in optimal cutting temperature (OCT) compound (SAKURA, OH, USA) followed by slicing into 9 μm coronal sections for further immunofluorescence and Nissl staining analysis.

For immunofluorescence staining [25], slides were warmed at room temperature for 30 min, washed with PBS, blocked with QuickBlot™ Blocking Buffer for immunofluorescence (Beyotime, Shanghai, China, Cat. No. P0260) for 1 h at room temperature, and then incubated at 4°C overnight with primary antibodies including mouse anti-NeuN (1 : 500, Abcam, Cambridge, UK, Cat. No. ab-104224), goat anti-Iba-1 (1 : 500, Abcam, Cambridge, UK, Cat. No. ab-5076), mouse anti-GFAP (1 : 500, Abcam, Cambridge, UK, Cat. No. ab10062), rabbit anti-Nurr1 (1 : 100, Bioss, Beijing, China, Cat. No. bs-20744r), and rabbit anti-IL-1β (1 : 100, Abcam, Cambridge, UK, Cat. No. ab9722). After warming at room temperature for 30 min, the slides were washed with PBS, incubated at room temperature for 2 h with secondary antibodies, and labeled cell nuclei with DAPI Fluoromount-G™ (YEASEN, Shanghai, China, Cat. No. 36308ES20).

For Nissl staining [26], slides were incubated with 0.5% cresyl violet (Sigma-Aldrich, St. Louis, MO, USA) solution at room temperature for 30 min, dehydrated with ethanol absolute, and sealed with a neutral resin containing xylene.

2.5. Western Blot. Total extracts of the brain and cells were lysed using RIPA lysis buffer (Beyotime, Shanghai, China, Cat. No. P0013B), while nuclear and cytoplasmic proteins were extracted using Nuclear and Cytoplasmic Protein Extraction Kit (Beyotime, Shanghai, China, Cat. No. P0027).

Western blot was operated as previously reported [27]. Briefly, proteins were appropriately separated by SDS-polyacrylamide gel electrophoresis and then transferred into

the PVDF membrane. After blocking with QuickBlot™ Blocking Buffer for western blot (Beyotime, Shanghai, China, Cat. No. P0252) 1 h at room temperature, the membrane was incubated at 4°C overnight with primary antibodies including mouse anti-β-actin (1 : 5000, Proteintech, Hubei, China, Cat. No. 60008-1-Ig), mouse anti-histone H3 (1 : 1000, Cell Signaling Technology, MA, USA, Cat. No. 9715), rabbit anti-Nurr1 (1 : 1000, Proteintech, Hubei, China, Cat. No. 10975-2-AP), rabbit anti-ZO-1 (1 : 100, Santa Cruz, TX, USA, Cat. No. sc-33725), rabbit anti-claudin-5 (1 : 100, Santa Cruz, TX, USA, Cat. No. sc-28670), rabbit anti-occludin (1 : 100, Santa Cruz, TX, USA, Cat. No. sc-133256), rabbit anti-MMP9 (1 : 100, Abcam, Cambridge, UK, Cat. No. ab38898), and rabbit anti-NF-κB p65 (1 : 1000, Cell Signaling Technology, MA, USA, Cat. No. 8242). Subsequently, the membrane was incubated with horseradish peroxidase-conjugated goat anti-rabbit or mouse secondary antibodies for 1 h at room temperature, and visualized by ECL Plus chemiluminescence reagent kit (Amersham Bioscience, Arlington Heights, IL). The densities of bands were quantified with software ImageJ (NIH).

2.6. RNA Extraction and qRT-PCR. The total RNA of tissues and cells was extracted using TRIzol™ Reagent (Life Technologies, CA, USA, Cat. No. 15596018). The single-stranded cDNA was synthesized at 37°C for 15 min followed 85°C 5 s by using Evo M-MLV Reverse Transcriptase (Accurate Biotechnology, Hunan, China, Cat. No. AG11605). The qRT-PCR was performed using SYBR® Green Premix Pro Taq HS qPCR Kit (Accurate Biotechnology, Hunan, China, Cat. No. AG11701) in Applied Biosystems 7500 Real-Time PCR System (Life Technologies, CA, USA) as follows: 95°C 20 s, 40 cycles of amplification at 95°C 3 s and 60°C 30 s. All qRT-PCR were conducted at least 3 technical replicates and 3 biological replicates. The relative expression of targeted genes was normalized to β-actin and analyzed using the $2^{-\Delta\Delta Ct}$ method. The primers of targeted genes are listed in Supplementary Table 1.

2.7. SAH Model In Vitro. Following SAH, the erythrocytes lyse and release their hemoglobin, which degrades to hemin (Fe^{3+} protoporphyrin IX). The toxicity of hemin occurs after it has been taken up into cells and thereby causes various harmful responses such as inflammation and oxidative stress [28]. Hence, we stimulated HT22 cells by administrating 200 μM hemin (Sigma-Aldrich, MO, USA, Cat. No. H9039) to induce the SAH model in vitro. Meanwhile, cells were treated with AQ (0 μM, 1 μM, 5 μM, 10 μM, and 30 μM) or vehicles [29].

For cell viability, HT22 cells (40000/mL) were seeded in a 96-well plate and cocultured with hemin and AQ. After washing extensively with PBS, cells were cultured with 10% CCK-8 (BOSTER, Wuhan, China, Cat. No. AR1199) for 1 h and measured at 450 nm by a microplate reader (BioTek, USA) to obtain OD value.

For apoptosis and necrosis analysis, HT22 cells (100000/mL) were cultured in a 6-well plate and subjected to hemin and AQ. After trypsinized, HT22 cells were centrifuged and resuspended in 100 μL binding buffer. HT22 cells were incubated with 4 μL Annexin V-FITC for 10 min at room temperature and then incubated with 4 μL PI for 5 min at room temperature. HT22 cell suspensions were added 400 μL PBS before analyzed by flow cytometry. Annexin V-FITC$^+$, PI$^+$/Annexin V-FITC$^-$, and PI$^-$/Annexin V-FITC$^-$ were determined as apoptosis, necrosis, and survival cells, respectively. All the reagents involved were purchased from Solarbio (Cat. No. CA1020).

For the effects of the neuron on microglia [30], HT22 cells were treated with hemin or AQ as described above, washed extensively with PBS, and cultured in a nonstimulated condition for 24 h. The culture was collected and centrifuged to obtain supernatant culture. Subsequently, BV2 cells were treated with the supernatant culture and harvested for qPCR analysis.

2.8. Statistical Analysis. Data were analyzed by SPSS software 22.0 and visualized by GraphPad Prism software 8.0. The normal distribution and variance homogeneity of data were tested by the Shapiro-Wilk and Levene methods, respectively. When meeting normal distribution and homogeneity of variance, data were analyzed by Student's t-test for two groups or one-way analysis of variance (ANOVA) with Tukey's post hoc contrasts for multigroups. Otherwise, the Mann–Whitney nonparametric test and Kruskal-Wallis test with post hoc contrast by the Dunn-Bonferroni test were introduced to compare the difference. Multiple groups' mortality rates were compared by the chi-square tests followed by post hoc contrast using the Bonferroni method.

3. Results

3.1. AQ Improved the Outcomes and Alleviated Blood-Brain Barrier (BBB) Disruption after SAH. After SAH models induced 24 h, no significant difference in bleeding volume was observed between the SAH+vehicle and SAH+AQ groups (Figures 1(a) and 1(b)). The mortality rates were 0.00% (0/24), 36.84% (14/38), and 17.24% (5/29) in the sham, SAH+vehicle, and SAH+AQ groups, respectively (Figure 1(c)). The weight loss ratio was higher in the SAH+vehicle group than that in the SAH+AQ group (Figure 1(d)). Moreover, the administration of AQ could significantly increase the modified Garcia score and beam score (Figures 1(e) and 1(f)).

Subsequently, we investigated the BBB disruption. Compared with the sham group, the water content of the left and right hemispheres of the SAH+vehicle group dramatically elevated while declined in the SAH+AQ group (Figure 1(g)). Besides, we analyzed the level of tight junction proteins involving in maintaining the integrity of BBB. The downregulation of ZO-1, occludin, and claudin-5 caused by SAH was greatly inhibited by the treatment of AQ (Figures 1(h)–1(k)).

3.2. Nurr1 Mainly Expressed in Neuron after SAH. Since AQ was an agonist of Nurr1, we analyzed the location of Nurr1 by double labeling Nurr1 with NeuN, Iba-1, and GFAP facilitating for further exploring the mechanism of AQ on SAH. The quantitative analysis showed that Nurr1$^+$NeuN$^+$ cells were 96.78%, 83.61%, and 89.43% and Nurr1$^+$NeuN$^-$ cells were 3.21%, 16.39%, and 11.97% in the sham, SAH+vehicle,

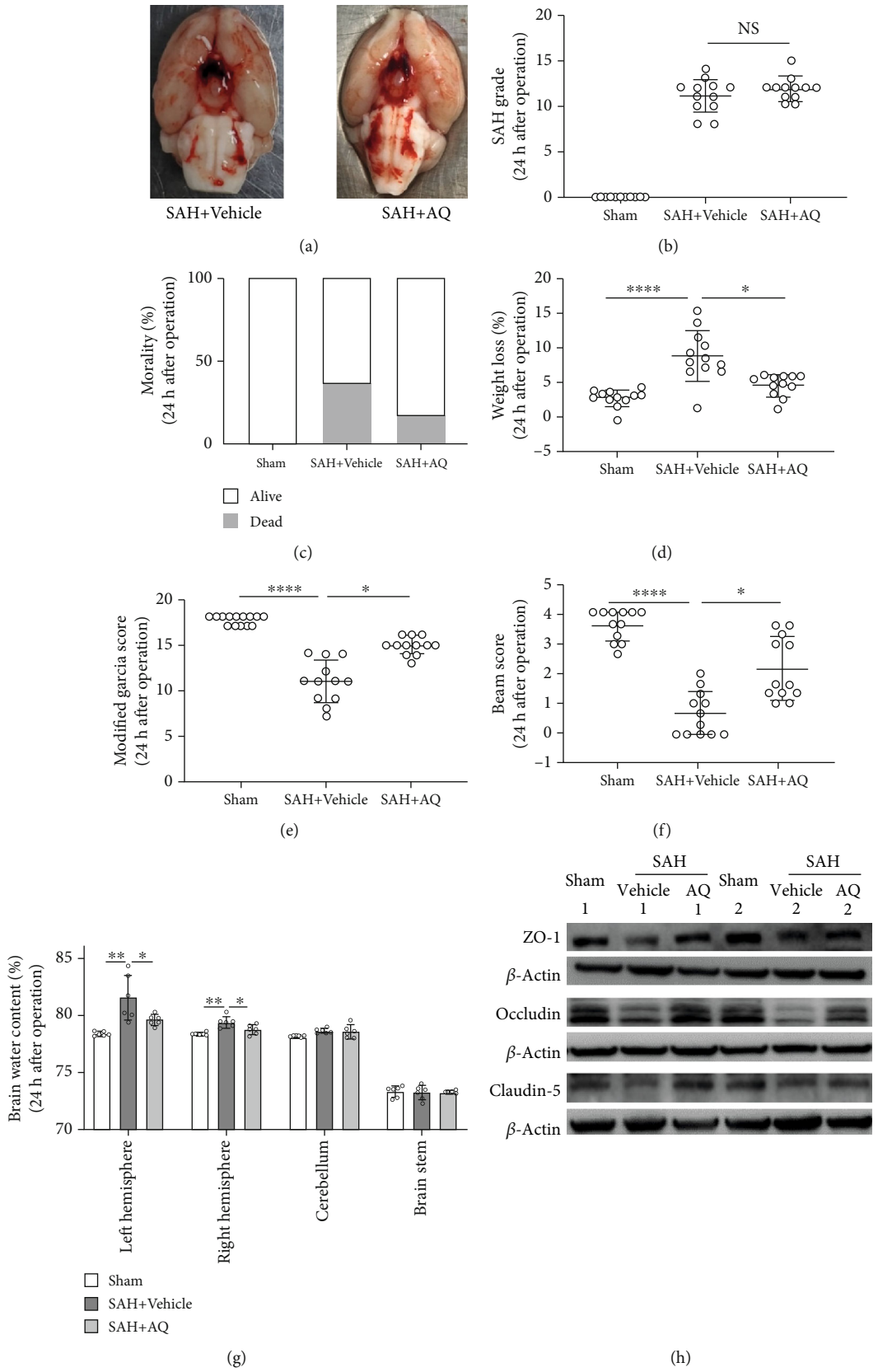

Figure 1: Continued.

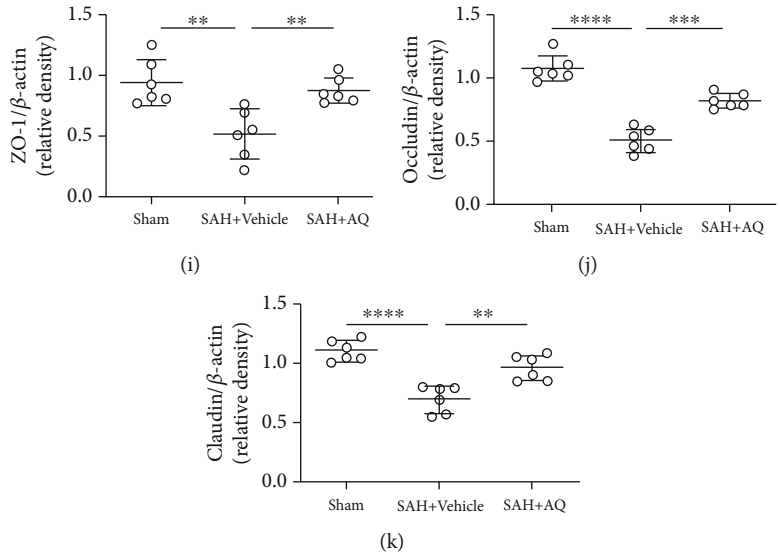

Figure 1: Effect of AQ on outcomes and brain edema. (a) Representative brain samples were harvested from the SAH+vehicle and SAH+AQ groups. (b) Hemorrhage volume quantified by SAH grade. $n = 12$ per group. (c, d) Mortality rate and weight loss were assessed among the sham, SAH+vehicle, and SAH+AQ groups. $n = 12$ per group. (e, f) Neurological function assessed via modified Garcia score and beam score. $n = 12$ per group. (g) The water content of the left hemisphere, right hemisphere, cerebellum, and brain stem. $n = 6$ per group. (h–k) Representative western blot bands and relative quantification of the protein expression of ZO-1, occludin, and claudin-5. $n = 6$ per group. NS: no significance; $^{*}p < 0.05$, $^{**}p < 0.01$, $^{***}p < 0.001$, and $^{****}p < 0.0001$.

and SAH+AQ groups, respectively, which indicated that Nurr1 expressed mainly in the neuron other than microglia and astrocytes (Figures 2(a)–2(c), Supplementary Figure 1).

3.3. Stimulation of Nurr1 with AQ Attenuated Neuron Injury. To assess the neuron injury, we performed the Nissl staining and analyzed the three regions (CA1, CA3, and DG) of the hippocampus and cortex among the groups [31]. Compared with sham, a mass of deeply stained neurons with shrunken cell bodies, characters of damaged neurons [32], were observed after SAH induced 24 h, while more lightly stained with larger cell bodies, characters of viable neurons [32], were observed after administration with AQ (Figure 3(a)). We next intervened HT22 cells with hemin and different doses of AQ and then analyzed the cell viability via CCK-8 at 6 and 24 h (Figure 3(b)). When the concentration was lower than 10 μM, the protective effect of AQ on HT22 cells was dose-dependent in different time points; however, the protective effect of AQ was reversed when the concentration was raised to 30 μM (Figure 3(c)). Herein, we applied the concentration gradients of 1, 5, and 10 μM in further studies with discard of the concentration of 30 μM. Subsequently, we investigated the apoptosis and necrosis of HT22 cells at 24 h. Similar to CCK-8, AQ reduced the percentage of apoptosis and necrosis while increased the percentage of survival cells (Figure 3(d)).

3.4. Stimulation of Nurr1 with AQ Inhibited the Proinflammatory Microglia/Macrophage and Alleviated the Neuroinflammation. Numerous researches had been demonstrated the key role of Nurr1 in anti-inflammation in multibrain diseases [10, 13, 33, 34]. We thus investigated the amount of proinflammatory phenotype of microglia/macrophage and the inflammation response. Following SAH, the microglia/macrophage increased and mostly transformed to activated phenotypes with larger soma size and shorter protrusions [35], compared to the SAH +AQ and sham groups (Figure 4(a)). Moreover, treatment with AQ decreased the number of IL-1β^{+} microglia/macrophage (Figure 4(a)), which was consistent with the mRNA level of IL-1β, CD68, CD86, and TNF-α (Figure 4(b)).

3.5. Stimulation of Nurr1 with AQ Inhibited the Proinflammatory Microglia Promoted by Damage Neurons Secreting MMP9. Emerging studies have shown that neurons (notably damage neurons) were not only passive targets in diseases but they also played an active role by secreting cytokines to accelerate microglial activation and inflammatory response [36, 37]. Based on the protective effect of AQ on neurons, we assumed that AQ could inhibit microglia activation and the accompanying inflammation by reducing harmful cytokines secreted from damaged neurons. After stimulating BV2 cells with supernatant from HT22 cells, we found the inflammation cytokines (IL-1β and TNF-α) and the M1-like phenotype markers (CD68 and CD86) were downregulated on a dose-dependent manner after treatment with AQ (Figure 5(a)). Subsequently, we detected the expression level of MMP9 in HT22 cells, a classic cytokine secreted from neurons to influence the activities of microglia, and observed the great upregulation after hemin stimulation while downregulated dose-dependently by treating with AQ (Figure 5(b)).

3.6. AQ Reduced Nuclear NF-κB by Activating Nurr1. As a nuclear receptor, Nurr1 mainly functioned in the nucleus.

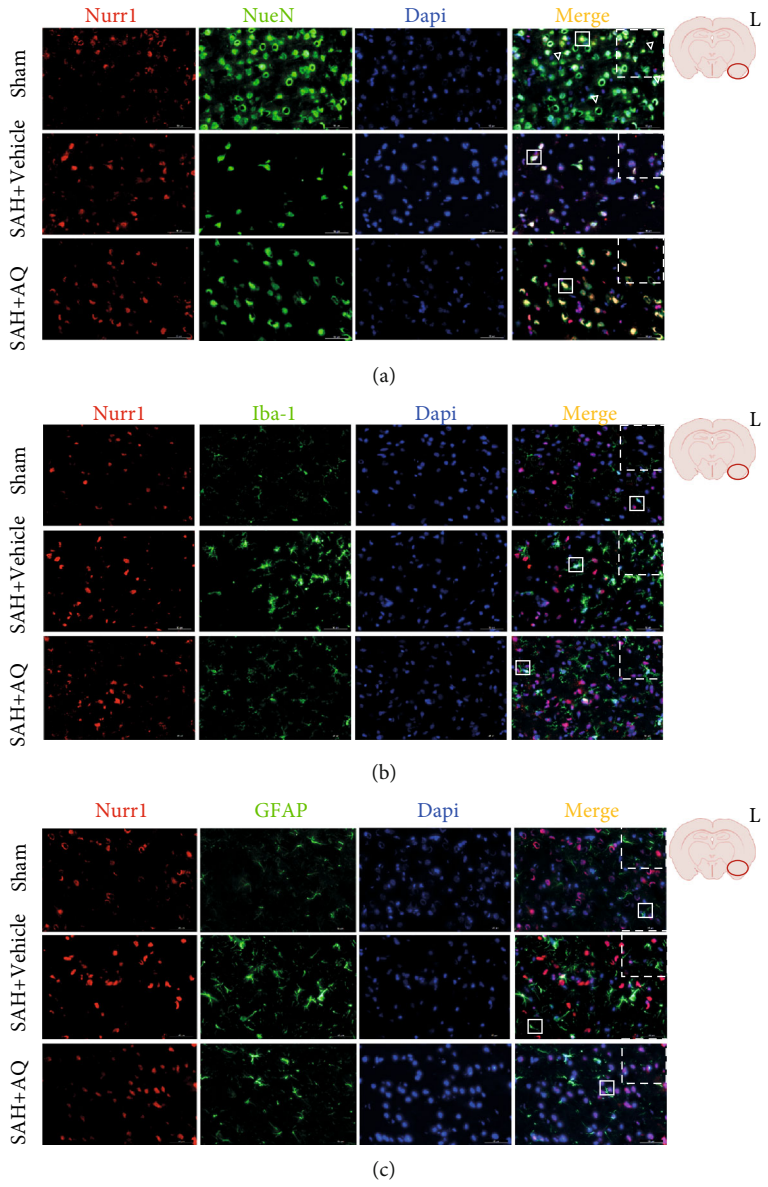

Figure 2: Distribution of Nurr1. Representative immunofluorescence images showed the localization of Nurr1 with (a) NeuN, (b) Iba-1, and (c) GFAP. Scale bar = 50 μm.

Hence, we investigated the nuclear expression of Nurr1. Compared with sham, the nuclear expression of Nurr1 was significantly increased in the SAH+vehicle group, but reduced in the SAH+AQ group (Figure 6(a)). A similar phenomenon was observed in the HT22 cells; moreover, the effect of AQ on the expression of nuclear Nurr1 was in a dose-dependent manner (Figure 6(c)). Numerous studies had reported that Nurr1 exerted an anti-inflammatory effect by regulating NF-κB in vitro and in vivo [38–40]. The stimulation of Nurr1 with AQ could decrease the expression of nuclear NF-κB in the rat models and HT22 cells (Figures 6(a) and 6(c)). Several studies demonstrated the subcellular translocation of nuclear receptors upon the stimulations, including PPAR [41] and RXR [42]. Hence, we detected the cytoplasmic expression of Nurr1 and observed that the cytoplasmic expression of Nurr1 was reduced in the SAH+vehicle group while increased in the SAH+AQ group compared to the sham group (Figure 6(b)), which was consistent with the results in vitro (Figure 6(d)).

4. Discussion

As we have known, this is the first study that investigated the effect of AQ on SAH. Here, we investigated the role and mechanisms of Nurr1 and its agonist (AQ) in the context of SAH, and made several major findings as follows: (1) AQ activated Nurr1 improved the outcome of rats and alleviated brain edema after SAH; (2) Nurr1 mostly expressed in the neuron and AQ could protect neuron both in vivo and in vitro models of SAH; (3) AQ inhibited the proinflammatory microglia/macrophage and the mechanisms may be

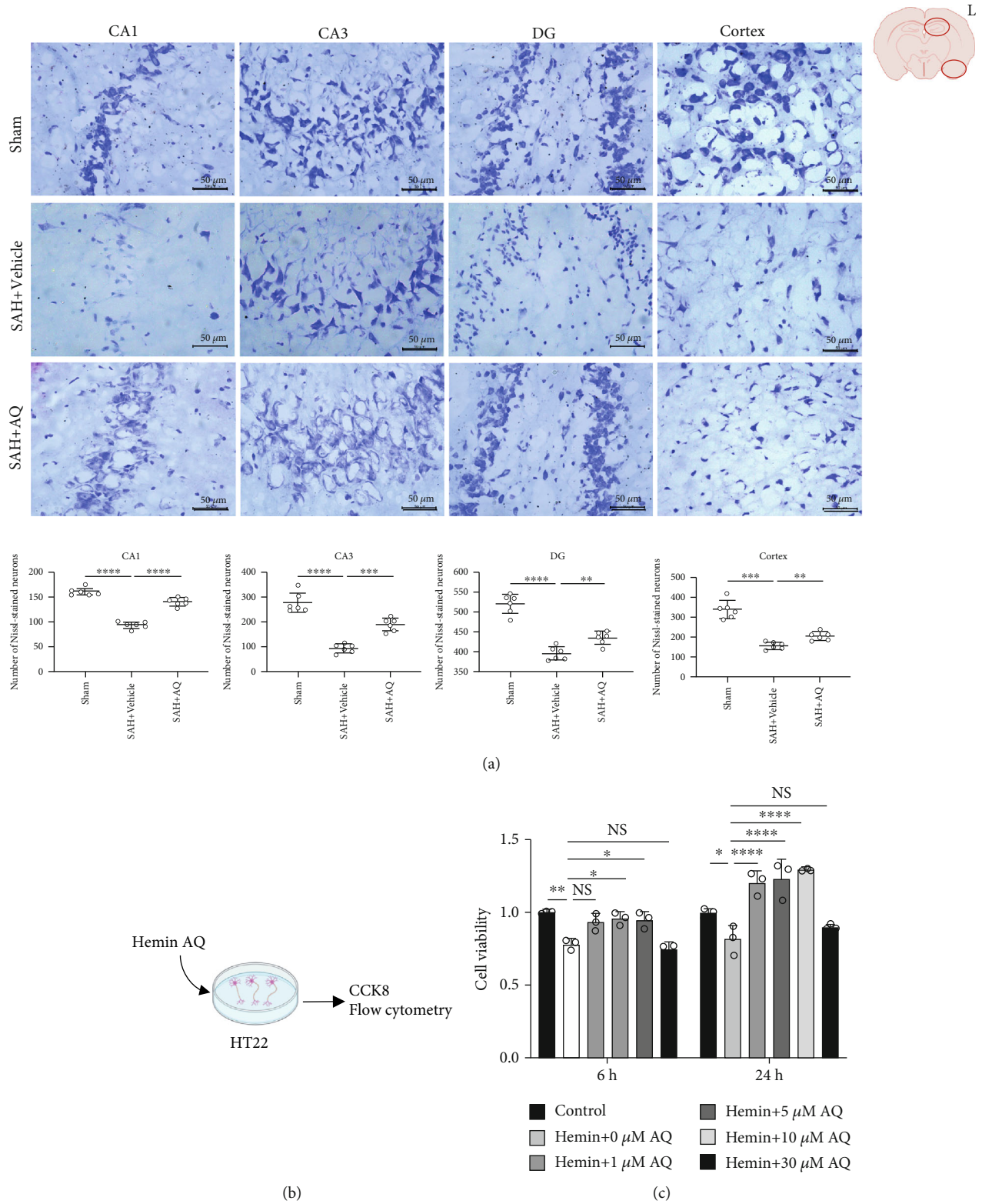

Figure 3: Continued.

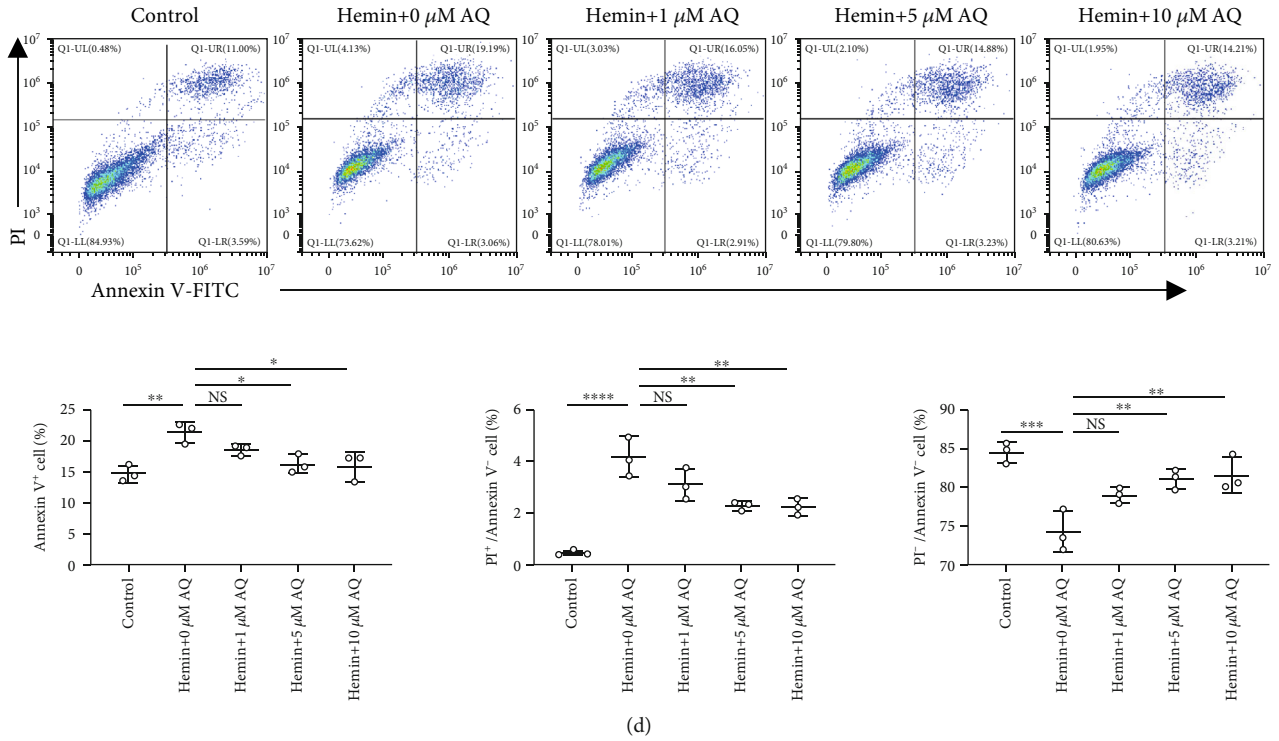

Figure 3: Effect of AQ on neuron protection. (a) Representative Nissl staining images of CA1, CA3, DG, and cortex and the corresponding quantification of the number of the neurons. $n = 6$ per group, scale bar = 50 μm. (b) Schematic diagram of CCK-8 and flow cytometry. (c) HT22 cell viability was assessed by CCK-8 at 6 and 24 hours after the intervention. $n = 3$ per group. NS: no significance; $^{*}p < 0.05$, $^{**}p < 0.01$, $^{***}p < 0.001$, and $^{****}p < 0.0001$. (d) HT22 cell apoptosis and necrosis were assessed by flow cytometry at 24 hours after the intervention. $n = 3$ per group. NS: no significance; $^{*}p < 0.05$, $^{**}p < 0.01$, and $^{***}p < 0.001$.

associated with the Nurr1/NF-κB/MMP9 pathway in the neuron (Figure 7).

Pharmaceutical stimulation Nurr1 with AQ showed a decrease of weight loss and brain edema while an increase of the neurological score, which indicated the protective effect of Nurr1 on SAH and the feasibility of AQ for the treatment of SAH. To clarify the mechanism of Nurr1, we explored the distribution of Nurr1. Consistent with Moon et al. [11], our immunofluorescence double-labeling experiment showed that Nurr1 was almost costained with the neuron, rather than microglia/macrophage or astrocyte. In general, neuron damage and death happened in early stage and at multiareas after SAH and were significantly associated with the prognosis [43–45]. Therefore, we considered that pharmacological activation of Nurr1 could reduce neuron injury, and this was confirmed by Nissl staining in vivo and CCK-8 and flow cytometry in vitro, which furthermore demonstrated the general neuroprotective effect of Nurr1 in multidiseases.

Despite Nurr1 was mainly expressed on neurons, bodies of literature had recently reported the antineuroinflammatory effects of Nurr1 in various disease models [34, 40, 46]. Meanwhile, taken into account that neuroinflammation was an important pathophysiological process involved in the early brain injury of SAH so that we could not ignore this point. By double labeling IL-1β and Iba-1, we observed a decrease in the percentage of IL-1β-positive microglia/macrophage after AQ intervention, which was similar to qPCR results. The data indicated that the anti-inflammatory effect of Nurr1 was also applicable to SAH. Generally speaking, the polarization of resting microglia/macrophage into proinflammatory microglia/macrophage was regulated by numerous factors, but it could be roughly divided into direct stimulation and indirect stimulation. For indirect stimulation, it was mainly the regulation of neuron or astrocyte on the activity of microglia. It was reported that modulation of microglia by neuron is through contact-dependent (such as CD200-CD200R, CX3CL1-CX3CR1, and TREM2L-TREM2) and contact-independent (such as CX3CL1 and MMP9) mechanisms [47, 48]. Additionally, exosomes derived from astrocyte modulated the phenotype of microglia [49]. Based on the distribution pattern of Nurr1, we focused on the interaction of neuron with microglia. After the intervention of microglia with cell culture supernatant obtained from neurons with avoidance the influence of hemin and AQ, we observed the inhibition of the expression of proinflammatory genes (IL-1β and TNF-α) and the M1-like phenotype markers (CD68 and CD86), which indicated that AQ could modulate the crosstalk between neuron and microglia. By detecting MMP9, a classical cytokine involved in the contact-independent mechanism [48], we found that the regulation of AQ on microglia activities may be related to its effects on the secretion of MMP9 from neurons.

Several studies had demonstrated that Nurr1 suppressed the gene expression of MMP9, but it did not seem to be through a directly transcriptional suppression mechanism [50–52]. Therefore, we focused on the nuclear NF-κB, a factor

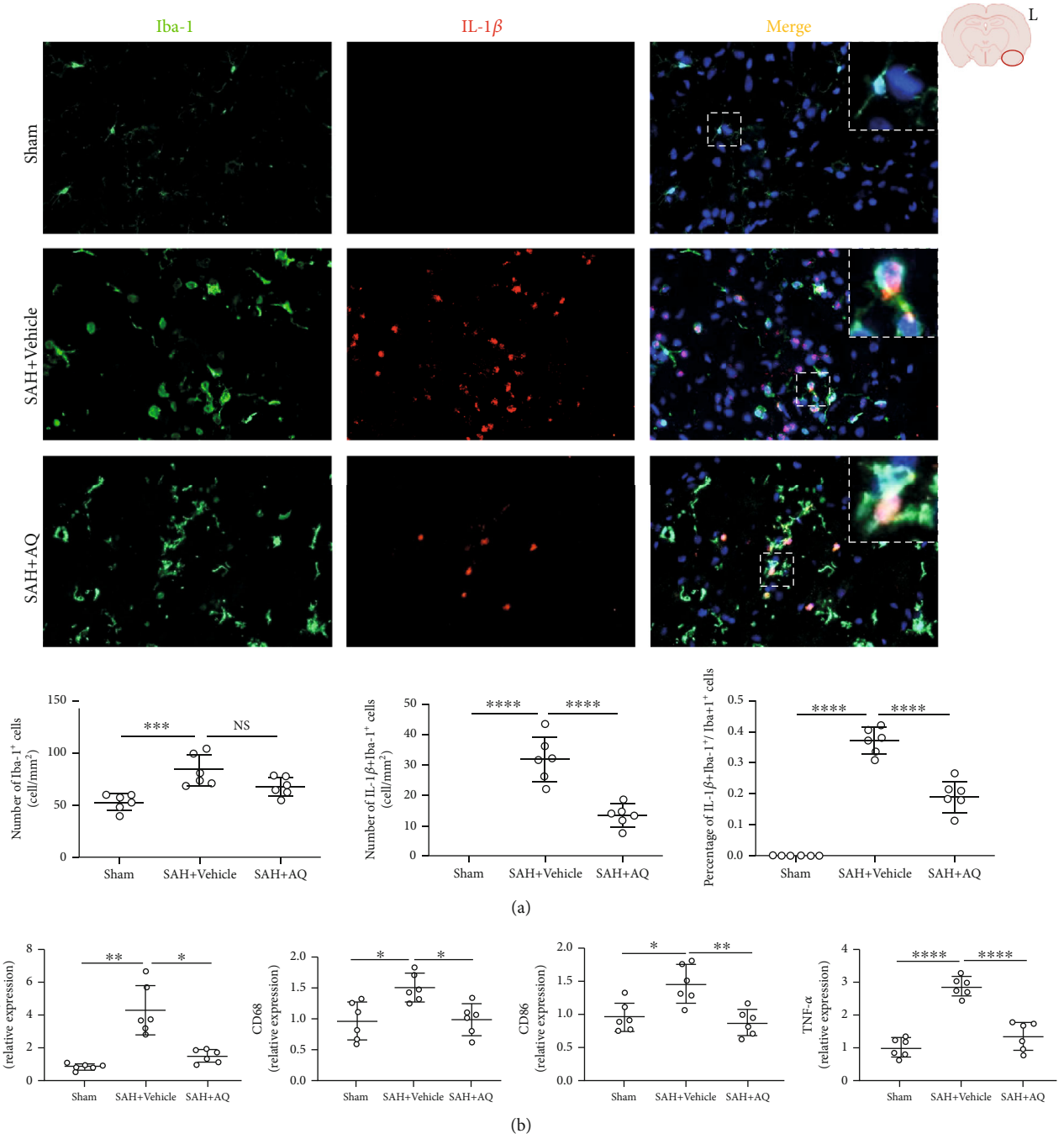

Figure 4: Effect of AQ on neuroinflammation. (a) Representative immunofluorescence images showed the morphology of Iba-1-positive cells and the corresponding quantification of the number of IL-1β^+/Iba-1$^+$ cells. $n = 6$ per group, scale bar = 50 μm. (b) The mRNA level of IL-1β, CD68, CD86, and TNF-α was assessed via qPCR. $n = 6$ per group. NS: no significance; $^*p < 0.05$, $^{**}p < 0.01$, $^{***}p < 0.001$, and $^{****}p < 0.0001$.

bridged the Nurr1 and MMP9 (Supplementary Figure 2), for it not only directly bound to the promoter of MMP9 [53, 54] but also directly interacted with Nurr1 [30, 55, 56]. Western blot results supported the reduced expression of nuclear NF-κB by treatment with AQ. Theoretically, after AQ intervention, nuclear Nurr1 would increase to maintain the inhibitory effect on NF-κB. However, by analyzing the nuclear and cytoplasmic expression of Nurr1, we found that Nurr1 increased in the nucleus, but decreased in the cytoplasm after SAH, while it was reversed after AQ treatment. Miranda et al. reported that C-DIM12, an agonist of Nurr1, inhibited the transcription activities of NF-κB in the BV2 cells; however, C-DIM12 further increased the nuclear translocation of Nurr1 on the basis of LPS stimulation [55], which was different from our results. The underlying reasons may be (1) different pharmacological mechanisms of the agonist; (2) different stimulus and the

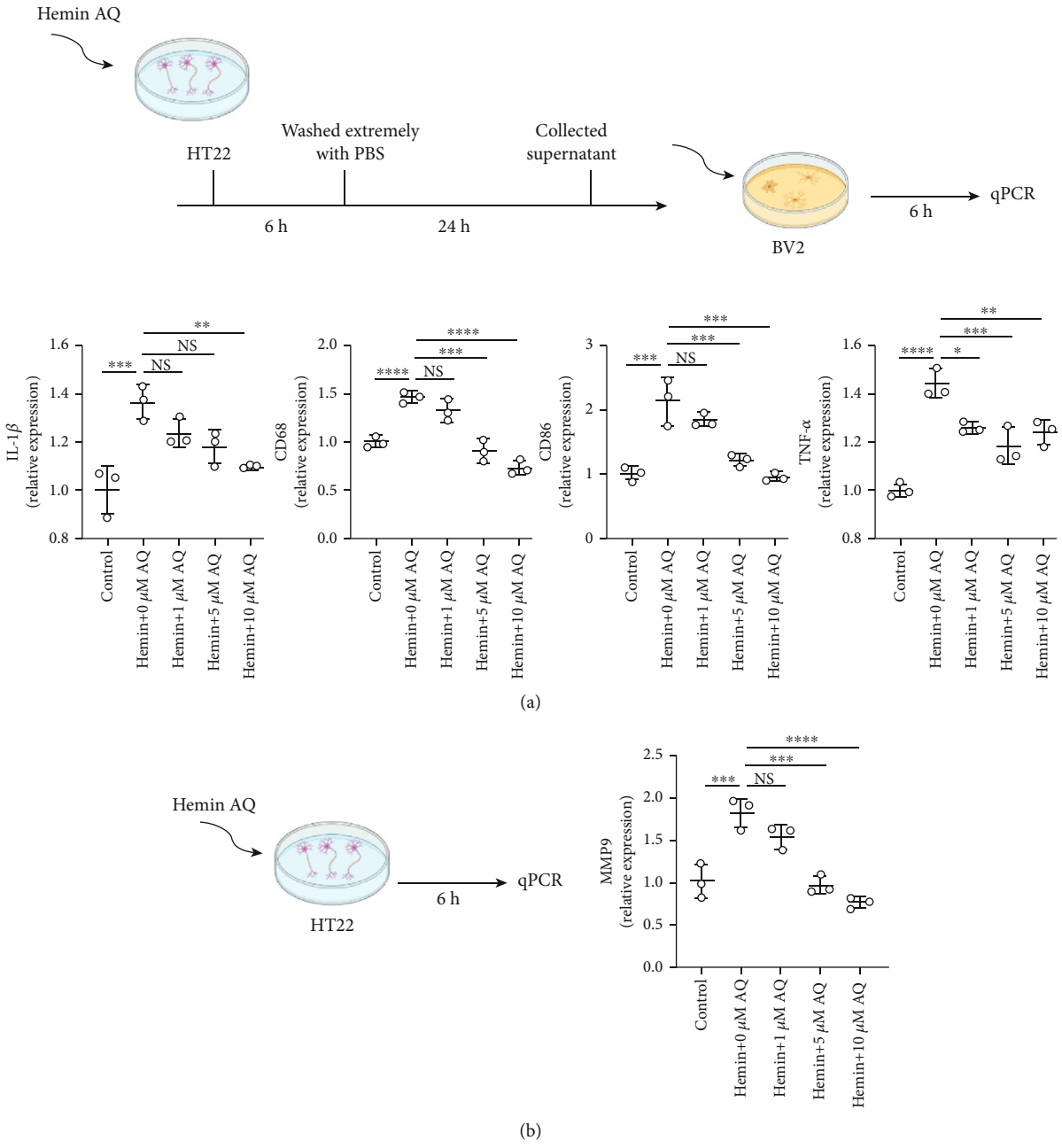

Figure 5: Effect of Nurr1 activation in neurons on the production of the inflammatory cytokines of microglia. (a) The upper part was the scheme of the experiment, and the lower part was the mRNA level of IL-1β, CD68, CD86, and TNF-α assessed via qPCR. $n = 3$ per group. (b) The left was the scheme of the experiment, and the right was the mRNA level of MMP9 assessed via qPCR. $n = 3$ per group. NS: no significance; $^{*}p < 0.05$, $^{**}p < 0.01$, $^{***}p < 0.001$, and $^{****}p < 0.0001$.

stimulation time; and (3) different cell types, which needed further studies. In any case, the data indicated that the subcellular translocation was essential for Nurr1 to exert its role. As a posttranslational modification, SUMOylation is involved in the regulation of protein subcellular localization [57, 58]. Saijo et al. demonstrated that the SUMOylation of Nurr1 was indispensable for the inhibition of the transcription activities of NF-κB [30]. Hence, it was reasonable to postulate that AQ regulated Nurr1 SUMOylation to promote it to bind to NF-κB and translocate the heterodimer to the cytoplasm for NF-κB degradation, which remained to be studied in the future.

This study still has the several following limitations. First, since there are no commercially available Nurr1 inhibitors and the abnormal behavior characteristics of Nurr1 knockout mice which may interfere with our neurobehavioral evaluation results [59], we did not verify our conclusion by inhibiting Nurr1. Second, we focused on the early brain injuries in the current study. The long-term function as well as the effect

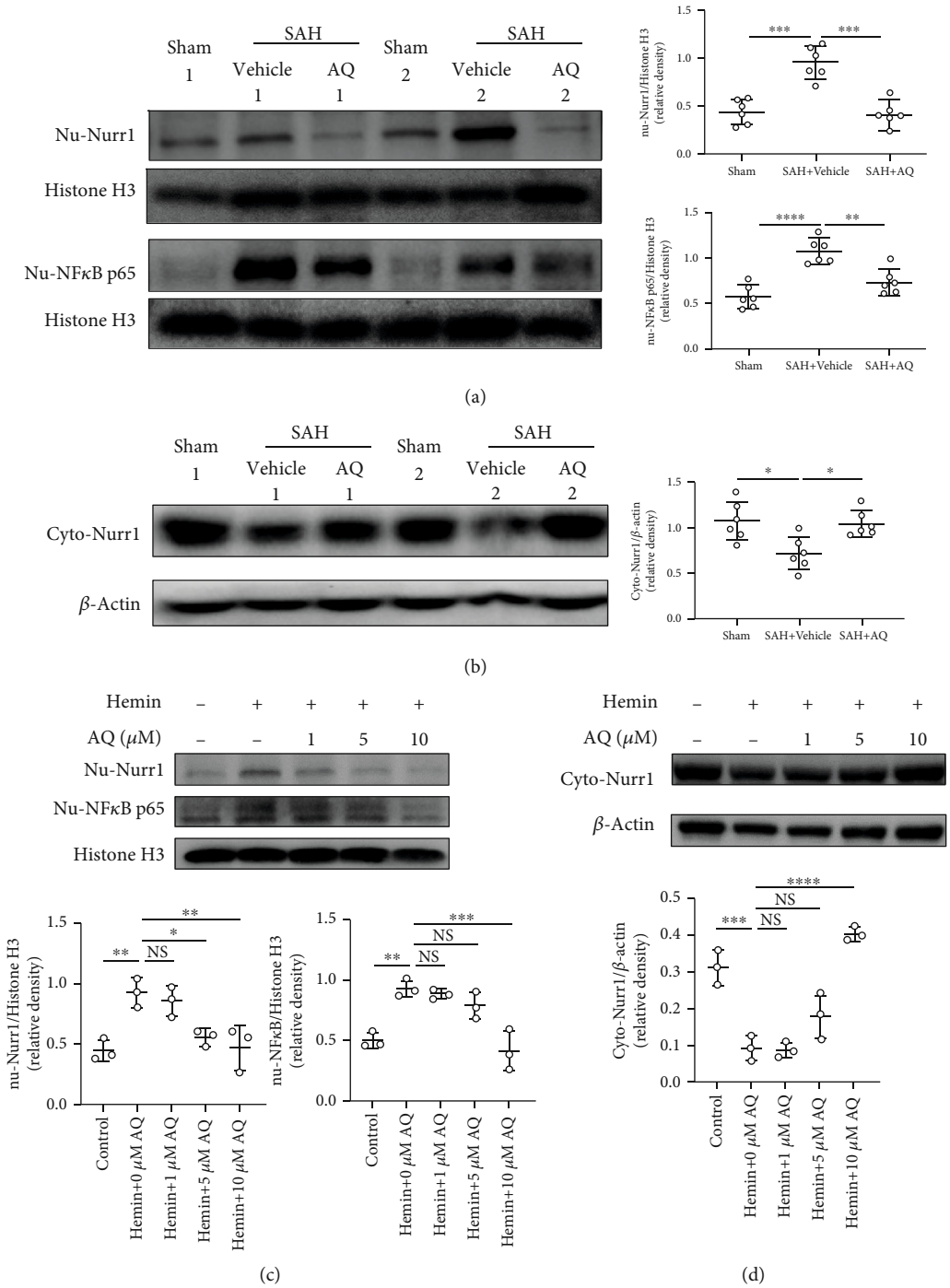

Figure 6: Effect of AQ on Nurr1 translocation and the expression of nuclear NF-κB. (a) Representative western blot bands and the quantification of the expression of nuclear Nurr1 and NF-κB p65 in rat models at 24 h after SAH. $n = 6$ per group. (b) Representative western blot bands and the quantification of the expression of cytoplasmic Nurr1 in rat models at 24 h after SAH. $n = 6$ per group. (c) Representative western blot bands and the quantification of the expression of nuclear Nurr1 and NF-κB p65 in HT22 cells at 6 h after the intervention. $n = 3$ per group. (d) Representative western blot bands and the quantification of the expression of cytoplasmic Nurr1 in HT22 cells at 6 h after the intervention. $n = 3$ per group. Nu: nuclear; Cyto: cytoplasmic; NS: no significance; $^{*}p < 0.05$, $^{**}p < 0.01$, $^{***}p < 0.001$, and $^{****}p < 0.0001$.

of different doses and the side effects of AQ especially in SAH should be performed in the follow-up research. Third, recent literature reported that Nurr1 had an anti-inflammatory effect on microglia. Based on the expression distribution of Nurr1, we mainly explained the anti-inflammatory effect of Nurr1 from another perspective, namely, the interaction between neurons and microglia in current study. Additionally, the specificity of the Nurr1/NF-κB/MMP9 axis in the anti-

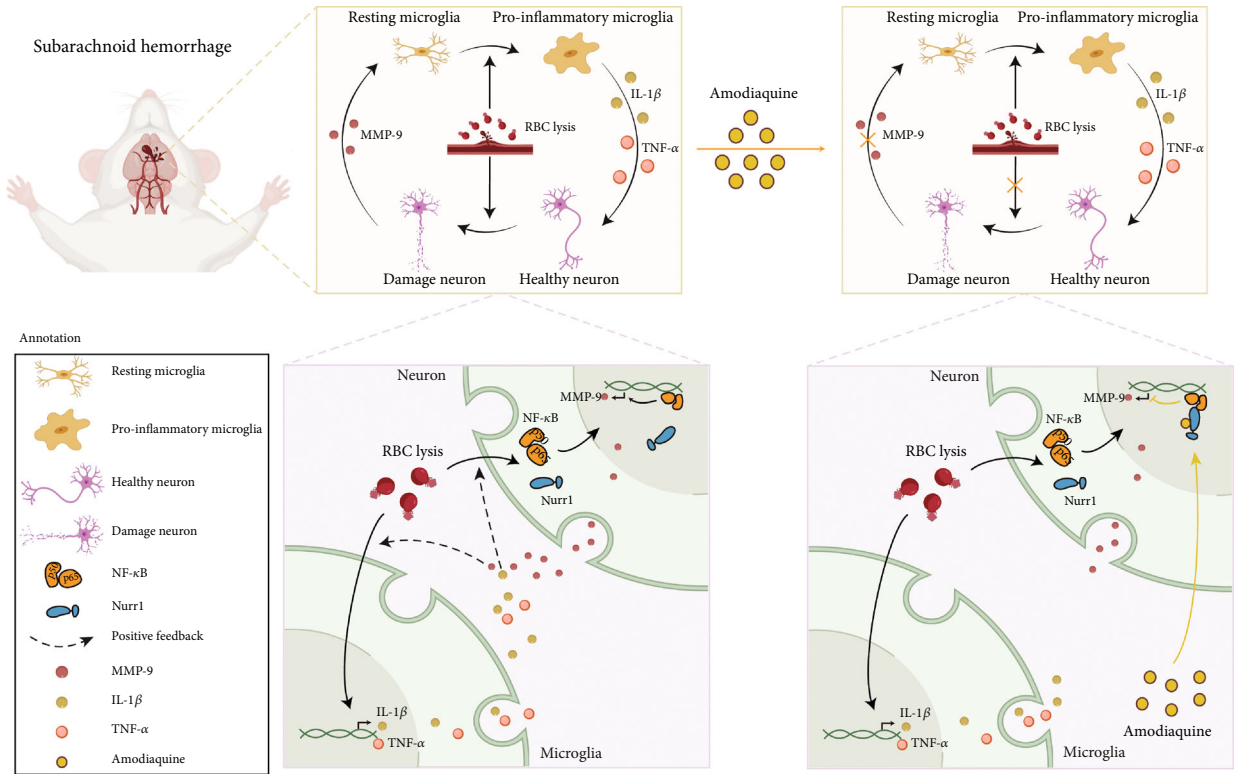

FIGURE 7: Illustrator of AQ functioned to protect neurons and reduce the neuroinflammation via a Nurr1/NF-κB/MMP9 pathway. The illustrator was created in assistance with BioRender (https://www.BioRender.com/).

inflammatory effect of Nurr1 in SAH, ICH, and other hemorrhagic stroke subtypes needs to be established in further study.

5. Conclusion

In summary, we confirmed that Nurr1 played an important role in the context of SAH and pharmacological stimulation of Nurr1 with AQ would be a promising treatment strategy based on the above data.

Data Availability

The raw data involved in the manuscript are available on reasonable request.

Conflicts of Interest

The authors declare that there is no conflict of interest.

Authors' Contributions

Jingyin Chen and Gao Chen conceived and designed the study. Huaijun Chen, Xiaobo Yu, and Libin Hu performed the SAH model and western blot and wrote the manuscript. Libin Hu and Yucong Peng performed the brain water content. Libin Hu, Hanhai Zeng, Yang Cao, Jianfeng Zhuang, Jianru Li, and Lin Wang performed the immunofluorescence staining and Nissl staining. Huaijun Chen, Qian Yu, Chaoran Xu, and Hang Zhou constructed the SAH model in vitro and performed the CCK-8 and flow cytometry. Yucong Peng, Xiongjie Fu, Guoyang Zhou, and Feng Yan performed the qPCR. Huaijun Chen and Xiaobo Yu analyzed the data and prepared the figures. All authors read, revised, and finally approved the manuscript. Huaijun Chen, Xiaobo Yu, and Libin Hu contributed equally to this work.

Acknowledgments

Figure 7 and the schematic diagram of a section of the brain in the Figures 2–4 was created using BioRender (http://www.BioRender.com/) and we appreciated it. This work was supported by the National Science Foundation of China (grant No. 81601003) and the Scientific Research Fund of Zhejiang Provincial Education Department (grant No. Y201941838).

Supplementary Materials

Supplementary Figure 1: quantification of $Nurr1^{+}NeuN^{+}$ and $Nurr1^{+}NeuN^{-}$ cells in the brains of the sham, SAH+vehicle, and SAH+AQ groups. Supplementary Figure 2: protein-protein interaction of Nurr1, NF-κB, and MMP9 downloaded from the STRING database (https://www.string-db.org/). Supplementary Table 1: sequence (5′-3′) of primers for qPCR. *(Supplementary Materials)*

References

[1] M. T. Lawton and G. E. Vates, "Subarachnoid hemorrhage," *The New England Journal of Medicine*, vol. 377, no. 3, pp. 257–266, 2017.

[2] S. Marbacher, B. Grüter, S. Schöpf et al., "Systematic review of in vivo animal models of subarachnoid hemorrhage: species, standard parameters, and outcomes," *Translational Stroke Research*, vol. 10, no. 3, pp. 250–258, 2019.

[3] T. Perlmann and A. Wallen-Mackenzie, "Nurr1, an orphan nuclear receptor with essential functions in developing dopamine cells," *Cell and Tissue Research*, vol. 318, no. 1, pp. 45–52, 2004.

[4] K. N. Alavian, S. Jeddi, S. I. Naghipour, P. Nabili, P. Licznerski, and T. S. Tierney, "The lifelong maintenance of mesencephalic dopaminergic neurons by Nurr1 and engrailed," *Journal of Biomedical Science*, vol. 21, no. 1, p. 27, 2014.

[5] J. Jankovic, S. Chen, and W. D. Le, "The role of Nurr1 in the development of dopaminergic neurons and Parkinson's disease," *Progress in Neurobiology*, vol. 77, no. 1-2, pp. 128–138, 2005.

[6] O. Saucedo-Cardenas, J. D. Quintana-Hau, W. D. le et al., "Nurr1 is essential for the induction of the dopaminergic phenotype and the survival of ventral mesencephalic late dopaminergic precursor neurons," *Proceedings of the National Academy of Sciences of the United States of America*, vol. 95, no. 7, pp. 4013–4018, 1998.

[7] P. Rivetti di Val Cervo, R. A. Romanov, G. Spigolon et al., "Induction of functional dopamine neurons from human astrocytes *in vitro* and mouse astrocytes in a Parkinson's disease model," *Nature Biotechnology*, vol. 35, no. 5, pp. 444–452, 2017.

[8] J. J. Song, S. M. Oh, O. C. Kwon et al., "Cografting astrocytes improves cell therapeutic outcomes in a Parkinson's disease model," *The Journal of Clinical Investigation*, vol. 128, no. 1, pp. 463–482, 2018.

[9] M. Moon, I. Jeong, C. H. Kim et al., "Correlation between orphan nuclear receptor Nurr1 expression and amyloid deposition in 5XFAD mice, an animal model of Alzheimer's disease," *Journal of Neurochemistry*, vol. 132, no. 2, pp. 254–262, 2015.

[10] F. Montarolo, S. Martire, S. Perga, and A. Bertolotto, "NURR1 impairment in multiple sclerosis," *International Journal of Molecular Sciences*, vol. 20, no. 19, p. 4858, 2019.

[11] M. Moon, E. S. Jung, S. G. Jeon et al., "Nurr1 (NR4A2) regulates Alzheimer's disease-related pathogenesis and cognitive function in the 5XFAD mouse model," *Aging Cell*, vol. 18, no. 1, article e12866, 2019.

[12] C. Merino-Zamorano, M. Hernández-Guillamon, A. Jullienne et al., "NURR1 involvement in recombinant tissue-type plasminogen activator treatment complications after ischemic stroke," *Stroke*, vol. 46, no. 2, pp. 477–484, 2015.

[13] S. Loppi, N. Kolosowska, O. Kärkkäinen et al., "HX600, a synthetic agonist for RXR-Nurr1 heterodimer complex, prevents ischemia-induced neuronal damage," *Brain, Behavior, and Immunity*, vol. 73, pp. 670–681, 2018.

[14] S. Pushpakom, F. Iorio, P. A. Eyers et al., "Drug repurposing: progress, challenges and recommendations," *Nature Reviews. Drug Discovery*, vol. 18, no. 1, pp. 41–58, 2019.

[15] G. Ciliberto, R. Mancini, and M. G. Paggi, "Drug repurposing against COVID-19: focus on anticancer agents," *Journal of Experimental & Clinical Cancer Research*, vol. 39, no. 1, p. 86, 2020.

[16] J. Dyall, E. A. Nelson, L. E. DeWald et al., "Identification of combinations of approved drugs with synergistic activity against Ebola virus in cell cultures," *The Journal of Infectious Diseases*, vol. 218, suppl_5, pp. S672–S678, 2018.

[17] C. H. Kim, B. S. Han, J. Moon et al., "Nuclear receptor Nurr1 agonists enhance its dual functions and improve behavioral deficits in an animal model of Parkinson's disease," *Proceedings of the National Academy of Sciences of the United States of America*, vol. 112, no. 28, pp. 8756–8761, 2015.

[18] R. C. Sellnow, K. Steece-Collier, F. Altwal et al., "Striatal Nurr1 facilitates the dyskinetic state and exacerbates levodopa-induced dyskinesia in a rat model of Parkinson's disease," *The Journal of Neuroscience*, vol. 40, no. 18, pp. 3675–3691, 2020.

[19] K. Kinoshita, K. Matsumoto, Y. Kurauchi, A. Hisatsune, T. Seki, and H. Katsuki, "A Nurr1 agonist amodiaquine attenuates inflammatory events and neurological deficits in a mouse model of intracerebral hemorrhage," *Journal of Neuroimmunology*, vol. 330, pp. 48–54, 2019.

[20] J. Chen, C. Qian, H. Duan et al., "Melatonin attenuates neurogenic pulmonary edema via the regulation of inflammation and apoptosis after subarachnoid hemorrhage in rats," *Journal of Pineal Research*, vol. 59, no. 4, pp. 469–477, 2015.

[21] T. Sugawara, R. Ayer, V. Jadhav, and J. H. Zhang, "A new grading system evaluating bleeding scale in filament perforation subarachnoid hemorrhage rat model," *Journal of Neuroscience Methods*, vol. 167, no. 2, pp. 327–334, 2008.

[22] J. H. Garcia, S. Wagner, K. F. Liu, and X. J. Hu, "Neurological deficit and extent of neuronal necrosis attributable to middle cerebral artery occlusion in rats. Statistical validation," *Stroke*, vol. 26, no. 4, pp. 627–635, 1995.

[23] T. Okada, B. Enkhjargal, Z. D. Travis et al., "FGF-2 attenuates neuronal apoptosis via FGFR3/PI3k/Akt signaling pathway after subarachnoid hemorrhage," *Molecular Neurobiology*, vol. 56, no. 12, pp. 8203–8219, 2019.

[24] J. Peng, Y. Zuo, L. Huang et al., "Activation of GPR30 with G1 attenuates neuronal apoptosis via src/EGFR/stat3 signaling pathway after subarachnoid hemorrhage in male rats," *Experimental Neurology*, vol. 320, p. 113008, 2019.

[25] H. Wang and M. P. Matise, "Immunofluorescence staining with frozen mouse or chick embryonic tissue sections," *Methods in Molecular Biology*, vol. 1018, pp. 175–188, 2013.

[26] Z. Wang, F. Zhou, Y. Dou et al., "Melatonin alleviates intracerebral hemorrhage-induced secondary brain injury in rats via suppressing apoptosis, inflammation, oxidative stress, DNA damage, and mitochondria injury," *Translational Stroke Research*, vol. 9, no. 1, pp. 74–91, 2018.

[27] T. Li, W. Xu, L. Gao et al., "Mesencephalic astrocyte-derived neurotrophic factor affords neuroprotection to early brain injury induced by subarachnoid hemorrhage via activating Akt-dependent prosurvival pathway and defending blood-brain barrier integrity," *The FASEB Journal*, vol. 33, no. 2, pp. 1727–1741, 2018.

[28] S. R. Robinson, T. N. Dang, R. Dringen, and G. M. Bishop, "Hemin toxicity: a preventable source of brain damage following hemorrhagic stroke," *Redox Report*, vol. 14, no. 6, pp. 228–235, 2013.

[29] S. Qiao, S. Tao, M. Rojo de la Vega et al., "The antimalarial amodiaquine causes autophagic-lysosomal and proliferative blockade sensitizing human melanoma cells to starvation- and chemotherapy-induced cell death," *Autophagy*, vol. 9, no. 12, pp. 2087–2102, 2014.

[30] K. Saijo, B. Winner, C. T. Carson et al., "A Nurr1/CoREST pathway in microglia and astrocytes protects dopaminergic neurons from inflammation-induced death," *Cell*, vol. 137, no. 1, pp. 47–59, 2009.

[31] W. Xu, J. Mo, U. Ocak et al., "Activation of melanocortin 1 receptor attenuates early brain injury in a rat model of subarachnoid hemorrhage viathe suppression of neuroinflammation through AMPK/TBK1/NF-κB pathway in rats," *Neurotherapeutics*, vol. 17, no. 1, pp. 294–308, 2020.

[32] D. Wu, N. Lai, R. Deng et al., "Activated WNK3 induced by intracerebral hemorrhage deteriorates brain injury maybe via WNK3/SPAK/NKCC1 pathway," *Experimental Neurology*, vol. 332, p. 113386, 2020.

[33] J. Dong, X. Liu, Y. Wang, H. Cai, and W. le, "Nurr1^{Cd11bcre} conditional knockout mice display inflammatory injury to nigrostriatal dopaminergic neurons," *Glia*, vol. 68, no. 10, pp. 2057–2069, 2020.

[34] M. Jakaria, M. E. Haque, D. Y. Cho, S. Azam, I. S. Kim, and D. K. Choi, "Molecular insights into NR4A2(Nurr1): an emerging target for neuroprotective therapy against neuroinflammation and neuronal cell death," *Molecular Neurobiology*, vol. 56, no. 8, pp. 5799–5814, 2019.

[35] K. S. Prabhakara, D. J. Kota, G. H. Jones, A. K. Srivastava, C. S. Cox Jr., and S. D. Olson, "Teriflunomide modulates vascular permeability and microglial activation after experimental traumatic brain injury," *Molecular Therapy*, vol. 26, no. 9, pp. 2152–2162, 2018.

[36] E. S. Wohleb, "Neuron-microglia interactions in mental health disorders: "for better, and for worse"," *Frontiers in Immunology*, vol. 7, p. 544, 2016.

[37] S. Marinelli, B. Basilico, M. C. Marrone, and D. Ragozzino, "Microglia-neuron crosstalk: signaling mechanism and control of synaptic transmission," *Seminars in Cell & Developmental Biology*, vol. 94, pp. 138–151, 2019.

[38] Q. H. Shao, W. F. Yan, Z. Zhang et al., "Nurr1: a vital participant in the TLR4-NF-κB signal pathway stimulated by α-synuclein in BV-2 cells," *Neuropharmacology*, vol. 144, pp. 388–399, 2019.

[39] B. J. Raveney, S. Oki, H. Hohjoh et al., "Eomesodermin-expressing T-helper cells are essential for chronic neuroinflammation," *Nature Communications*, vol. 6, no. 1, p. 8437, 2015.

[40] V. Valsecchi, M. Boido, F. Montarolo et al., "The transcription factor Nurr1 is upregulated in amyotrophic lateral sclerosis patients and SOD1-G93A mice," *Disease Models & Mechanisms*, vol. 13, no. 5, article dmm043513, 2020.

[41] T. Teratani, K. Tomita, S. Toma-Fukai et al., "Redox-dependent PPARγ/Tnpo1 complex formation enhances PPARγ nuclear localization and signaling," *Free Radical Biology & Medicine*, vol. 156, pp. 45–56, 2020.

[42] P. Lefebvre, Y. Benomar, and B. Staels, "Retinoid X receptors: common heterodimerization partners with distinct functions," *Trends in Endocrinology and Metabolism*, vol. 21, no. 11, pp. 676–683, 2010.

[43] X. Gao, Y. Xiong, Q. Li et al., "Extracellular vesicle-mediated transfer of miR-21-5p from mesenchymal stromal cells to neurons alleviates early brain injury to improve cognitive function via the PTEN/Akt pathway after subarachnoid hemorrhage," *Cell Death & Disease*, vol. 11, no. 5, p. 363, 2020.

[44] J. Zhao, X. Xiang, H. Zhang et al., "CHOP induces apoptosis by affecting brain iron metabolism in rats with subarachnoid hemorrhage," *Experimental Neurology*, vol. 302, pp. 22–33, 2018.

[45] Q. Zhao, X. Che, H. Zhang et al., "Thioredoxin-interacting protein links endoplasmic reticulum stress to inflammatory brain injury and apoptosis after subarachnoid haemorrhage," *Journal of Neuroinflammation*, vol. 14, no. 1, p. 104, 2017.

[46] S. G. Jeon, A. Yoo, D. W. Chun et al., "The critical role of Nurr1 as a mediator and therapeutic target in Alzheimer's disease-related pathogenesis," *Aging and Disease*, vol. 11, no. 3, pp. 705–724, 2020.

[47] L. Zhang, J. Xu, J. Gao, Y. Wu, M. Yin, and W. Zhao, "CD200-, CX3CL1-, and TREM2-mediated neuron-microglia interactions and their involvements in Alzheimer's disease," *Reviews in the Neurosciences*, vol. 29, no. 8, pp. 837–848, 2018.

[48] Y. Liu, M. Li, Z. Zhang, Y. Ye, and J. Zhou, "Role of microglia-neuron interactions in diabetic encephalopathy," *Ageing Research Reviews*, vol. 42, pp. 28–39, 2018.

[49] X. Long, X. Yao, Q. Jiang et al., "Astrocyte-derived exosomes enriched with miR-873a-5p inhibit neuroinflammation via microglia phenotype modulation after traumatic brain injury," *Journal of Neuroinflammation*, vol. 17, no. 1, p. 89, 2020.

[50] M. Jodeiri Farshbaf, M. Forouzanfar, K. Ghaedi et al., "Nurr1 and PPARγ protect PC12 cells against MPP+ toxicity: involvement of selective genes, anti-inflammatory, ROS generation, and antimitochondrial impairment," *Molecular and Cellular Biochemistry*, vol. 420, no. 1-2, pp. 29–42, 2016.

[51] R. Rodríguez-Calvo, B. Ferrán, J. Alonso et al., "NR4A receptors up-regulate the antiproteinase alpha-2 macroglobulin (A2M) and modulate MMP-2 and MMP-9 in vascular smooth muscle cells," *Thrombosis and Haemostasis*, vol. 113, no. 6, pp. 1323–1334, 2017.

[52] K. S. Mix, M. G. Attur, H. al-Mussawir, S. B. Abramson, C. E. Brinckerhoff, and E. P. Murphy, "Transcriptional repression of matrix metalloproteinase gene expression by the orphan nuclear receptor NURR1 in cartilage," *The Journal of Biological Chemistry*, vol. 282, no. 13, pp. 9492–9504, 2007.

[53] Y. F. Li, X. B. Xu, X. H. Chen, G. Wei, B. He, and J. D. Wang, "The nuclear factor-κB pathway is involved in matrix metalloproteinase-9 expression in RU486-induced endometrium breakdown in mice," *Human Reproduction*, vol. 27, no. 7, pp. 2096–2106, 2012.

[54] J. W. Rhee, K. W. Lee, D. Kim et al., "NF-kappaB-dependent regulation of matrix metalloproteinase-9 gene expression by lipopolysaccharide in a macrophage cell line RAW 264.7," *Journal of Biochemistry and Molecular Biology*, vol. 40, no. 1, pp. 88–94, 2007.

[55] B. R. de Miranda, K. A. Popichak, S. L. Hammond et al., "The Nurr1 activator 1,1-bis(3′-indolyl)-1-(p-chlorophenyl)-methane blocks inflammatory gene expression in BV-2 microglial cells by inhibiting nuclear FactorκB," *Molecular Pharmacology*, vol. 87, no. 6, pp. 1021–1034, 2015.

[56] K. A. Popichak, S. L. Hammond, J. A. Moreno et al., "Compensatory expression of Nur77 and Nurr1 regulates NF-κB–dependent inflammatory signaling in astrocytes," *Molecular Pharmacology*, vol. 94, no. 4, pp. 1174–1186, 2018.

[57] Y. Yang, Y. He, X. Wang et al., "Protein SUMOylation modification and its associations with disease," *Open Biology*, vol. 7, no. 10, p. 170167, 2017.

[58] J. M. Henley, T. J. Craig, and K. A. Wilkinson, "Neuronal SUMOylation: mechanisms, physiology, and roles in neuronal dysfunction," *Physiological Reviews*, vol. 94, no. 4, pp. 1249–1285, 2014.

[59] F. Montarolo, S. Martire, S. Perga et al., "NURR1 deficiency is associated to ADHD-like phenotypes in mice," *Translational Psychiatry*, vol. 9, no. 1, p. 207, 2019.